

Lyman- α power spectrum as a probe of modified gravity

Philippe Brax,^a Patrick Valageas^a

^aInstitut de Physique Théorique, Université Paris-Saclay, CEA, CNRS,
F-91191 Gif sur Yvette, France

E-mail: philippe.brax@ipht.fr, patrick.valageas@ipht.fr

Abstract. We investigate the impact of modified-gravity models on the Lyman- α power spectrum. Building a simple analytical modeling, based on a truncated Zeldovich approximation, we estimate the intergalactic medium power spectrum and the Lyman- α flux decrement power spectrum along the line of sight. We recover the results of numerical simulations for $f(R)$ -gravity models and present new results for K-mouflage scenarios. We find that the shape of the distortion due to the modified gravity depends on the model, through the scale-dependence or not of their growth rate. This is more clearly seen in the three-dimensional power spectrum than in the one-dimensional power spectrum, where the line-of-sight integration smoothes the deviation. Whilst the Lyman- α power spectrum does not provide competitive bounds for $f(R)$ theories, it could provide useful constraints for the K-mouflage models. Thus, the efficiency of the Lyman- α power spectrum as a probe of modified-gravity scenarios depends on the type of screening mechanism and the related scale dependence it induces. The prospect of a full recovery of the three-dimensional Lyman- α power spectrum from data would also lead to stronger constraints and a better understanding of screening mechanisms.

Contents

1	Introduction	1
2	Modeling the Lyman-α flux decrement power spectrum	2
3	Modified-gravity scenarios	6
3.1	$f(R)$ theories	7
3.2	K-mouflage	9
4	Conclusion	11
A	The Zeldovich approximation	12

1 Introduction

Soon after the discovery of the acceleration of the expansion of the Universe, the possibility that modified gravity on cosmological scales could be at the origin of this late time acceleration was raised [1]. This led to a renewed interest in massive gravity [2, 3], which gives a tantalising link between the amount of dark energy necessary to generate the acceleration of the Universe and the graviton mass. Another class of models involving a new scalar field, akin to the scalar polarisation of massive gravity, could also lead to self-tuned [4] acceleration using the Horndeski [5, 6] (and beyond) [7] classification of trouble-free scalar theories in four dimensions. In both cases, the number of theories passing the stringent constraint on the speed of gravitational waves is extremely limited [8, 9]. In this paper, we shall focus on models which do not tackle the acceleration issue per se. They all contain a vacuum energy which is partially responsible for the late-time acceleration. On the other hand, gravity is still modified and constrained on large cosmological scales. We concentrate on models of the $f(R)$ type for which the astrophysical constraints imply that deviations from the Λ -CDM template are limited [10]. Nevertheless, for models of the K-mouflage type [11], where large clusters are not screened [12] and see the effects of the scalar field with no suppression, large-scale observables such as the Lyman- α forest are of relevance.

Such a type of modified gravity has mostly been studied on large linear scales through its impact on the cosmic microwave background (CMB) anisotropies (in particular the integrated Sachs-Wolfe effect), on weak lensing cosmic shear statistics, on the matter power spectrum; and on small nonlinear scales through the matter power spectrum, the abundance of virialized halos and clusters of galaxies. However, very few studies have considered the impact on the Lyman- α forest statistics, see for instance [13] for a work focusing on $f(R)$ -gravity using numerical simulations. In contrast, the Lyman- α power spectrum has become a useful probe of dark matter candidates [14–18] providing constraints on warm dark matter scenarios that suppress the matter power spectrum on small scales because of their non-negligible velocity dispersion. More generally, the Lyman- α power spectrum is a probe of the linear matter power spectrum and of the background cosmology [19–22]. Therefore, it is worth investigating whether the Lyman- α power spectrum could also provide useful constraints on modified gravity. In particular, to pass Solar System tests of gravity, modified-gravity scenarios must include screening mechanisms that ensure convergence to General Relativity in

high-density and small-scale environments. Depending on the model, screening may even apply up to galactic or cluster scales. In contrast, Lyman- α forest clouds, which correspond to weakly nonlinear density fluctuations and scales greater than virialized objects, should not be screened. Moreover, being in the weakly nonlinear regime, Lyman- α statistics could be better probes of the linear power spectrum than highly nonlinear scales, which are difficult to predict and involve complex effects, such as baryonic feedback or virialization processes, that can be degenerate with modified-gravity impacts or partly damp the sensitivity to linear modified-gravity effects. In addition, modified-gravity models often induce a new scale dependence for the matter power spectrum, which is typically enhanced as compared with the LCDM prediction instead of being suppressed as in warm dark matter scenarios, that could also modify the shape of the Lyman- α power spectrum.

In this paper, we present a first step to estimate the impact of modified-gravity scenarios on the Lyman- α power spectrum. We first build in section 2 a simple model for the Lyman- α power spectrum. It is based on a truncated Zeldovich approximation, which encodes the dependence on cosmology, and bias parameters that we keep fixed to simplify the analysis. We check that it provides a reasonable match to numerical simulations and observations, in the case of the concordance LCDM cosmology. Next, we apply this modeling to two modified-gravity scenarios in section 3. We check that we recover the results of numerical simulations [13] for $f(R)$ theories, and we present new results for K-mouflage models. We discuss the impact of these modified-gravity scenarios and we conclude in section 4.

2 Modeling the Lyman- α flux decrement power spectrum

Fitting formulas devised for the Lyman- α flux decrement δ_F usually express its power spectrum $P_{\delta_F}(\mathbf{k})$ in terms of the power spectrum $P_L(k)$ of the linear matter density contrast at the same redshift, multiplied by several cutoffs and amplification factors [18, 23]. These factors account for several effects, such as the bias between the neutral hydrogen gas distribution and the total matter distribution, thermal broadening, redshift-space distortions, the nonlinear growth of density fluctuations, ..., and are obtained from fits to numerical simulations. In this paper, we also use such cutoffs, which we do not accurately predict but have realistic orders of magnitude and are fitted to simulations and observations. However, we do not introduce an ad-hoc amplification factor and we model the effects associated with the nonlinearity of the underlying density field by an analytical model based on a truncated Zeldovich approximation. This scheme cannot reach the accuracy of dedicated hydrodynamical numerical simulations, but we can hope that it captures some of the dependence on the primordial matter power spectrum and the growth of large-scale density perturbations.

We follow the common description of the Lyman- α forest as due to fluctuations in a continuous intergalactic medium (IGM) [24–26] instead of a set of discrete objects. Thus, we first express the real-space IGM density power spectrum of the neutral hydrogen gas in terms of the primordial matter density power spectrum as

$$P_{\text{IGM}}(k) = P_{\text{Ztrunc}}(k) e^{-(k/k_J)^2}, \quad (2.1)$$

where $P_{\text{Ztrunc}}(k)$ is a truncated Zeldovich power spectrum [27–29] and k_J the Jeans wave number. We define this truncated Zeldovich power spectrum as the standard Zeldovich power spectrum $P_Z(k)$ associated with a truncated linear power spectrum $P_{\text{Ltrunc}}(k)$, instead of the genuine primordial linear power spectrum $P_L(k)$,

$$P_{\text{Ztrunc}} = \max_{k_{\text{trunc}}} P_Z[P_{\text{Ltrunc}}] \quad \text{with} \quad P_{\text{Ltrunc}}(k) = P_L(k)/(1 + k^2/k_{\text{trunc}}^2)^2. \quad (2.2)$$

An alternative approach would be to use a lognormal model for the IGM density field, written as $\delta_{\text{IGM}} \propto e^{\delta_L}$, and to use simulations to obtain the statistical properties of this lognormal field [24]. The advantage of our approach (2.1) is that it directly provides the power spectrum, without the need of numerical simulations.

It has been noticed for a long time that using a truncated linear power spectrum instead of the full linear power spectrum in the Zeldovich mapping provides a better description of large-scale structures; it actually fares better than both the linear and lognormal approximations [30]. Indeed, the initial power at high wavenumbers gives rise to artificially large displacements in the Zeldovich mapping, where particles simply follow their linear trajectories. This leads to particles moving beyond collapsed structures, instead of turning back and oscillating in gravitational potential wells, which gives rise to a steep free-streaming cutoff of the predicted nonlinear power spectrum, instead of the actual amplification associated with the collapse into virialized halos. Then, truncating the initial power at high k reduces this effect and enables one to recover the structure of the cosmic web [30]. Of course, such a scheme cannot describe the inner parts of the virialized halos. However, this is well suited to our purposes. Indeed, Lyman- α forest clouds consist of mildly nonlinear density fluctuations, typically associated with filaments or the outer parts of collapsed structures. Therefore, removing high-density collapsed regions is actually required to focus on the Lyman- α forest. Moreover, the maximization in Eq.(2.2) implies that the truncation wave number k_{trunc} that determines P_{Ltrunc} is defined as the one that maximizes $k^3 P_{\text{Ztrunc}}(k)$ at high k . Indeed, for large k_{trunc} , i.e. $k_{\text{trunc}} \gg k_{\text{NL}}$ where k_{NL} is the nonlinear transition scale with $\Delta_L^2(k) \sim 1$ ($\Delta^2 = 4\pi k^3 P$ is the logarithmic power that also measures the variance of density fluctuations at scale $1/k$), we recover the primordial linear power spectrum and the artificial smoothing of nonlinear structures. For small k_{trunc} , i.e. $k_{\text{trunc}} \ll k_{\text{NL}}$, we already remove power in the linear regime and prevent the formation of mildly nonlinear structures. For $k_{\text{trunc}} \sim k_{\text{NL}}$, we maximize the resulting Zeldovich power spectrum P_{Ztrunc} , which shows a universal tail $P_{\text{Ztrunc}}(k) \propto k^{-3}$, i.e. a flat $\Delta_{\text{Ztrunc}}^2(k)$ at high k . This captures the self-induced truncation of the mildly nonlinear density power spectrum we consider; the truncation is associated with the removal of high-density virialized regions, the formation of which is set by the onset of the nonlinear regime. This natural prescription also avoids introducing an additional free parameter k_{trunc} . This also ensures that the resulting power spectrum P_{Ztrunc} is not very sensitive to the form of the cutoff $1/(1 + k^2/k_{\text{trunc}}^2)^\nu$, where we could as well take $\nu = 1$ or 4 . Thus, we show in the left panel in Fig. 1 the power spectra obtained without truncation and with truncation, either with $\nu = 2$ (crosses) or $\nu = 4$ (squares). We can see that at redshift $z = 3$ the truncated Zeldovich approximation captures some of the nonlinear amplification of the matter density perturbations but saturates beyond $k_{\text{trunc}} \simeq 10h/\text{Mpc}$, as it does not describe the inner parts of collapsed halos. It mainly follows the standard Zeldovich approximation up to its peak and remains constant at higher k . We can check that the result is not sensitive to the exponent ν of the cutoff used for the truncation of the linear power spectrum.

Second, the cutoff $e^{-(k/k_J)^2}$ corresponds to the damping of density fluctuations in the gas by its nonzero pressure, with k_J the comoving Jeans wave number, which we define by the standard expressions [31, 32]

$$k_J = \frac{2\pi}{\lambda_J}, \quad \lambda_J \simeq \frac{1}{2.2} \frac{c_s}{a} \sqrt{\frac{\pi}{\mathcal{G}_N \bar{\rho}}}, \quad c_s = \sqrt{\frac{5k_B T}{3\mu m_p}}. \quad (2.3)$$

Here a is the scale factor, c_s the sound speed, $\mu \simeq 0.5$ the mean molecular weight, and we choose a typical temperature $T \sim 2 \cdot 10^4$ K. The factor 2.2 accounts for the fact that the Jeans

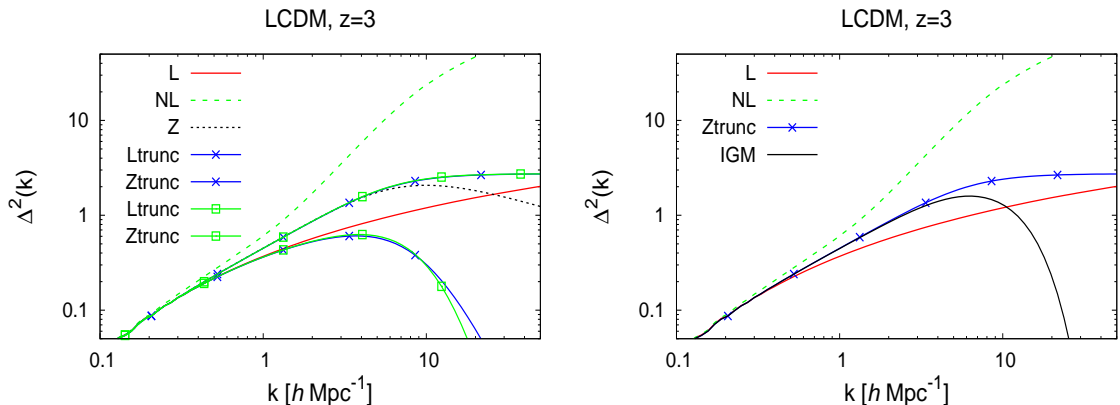


Figure 1. *Left panel:* logarithmic power $\Delta^2(k)$ for the linear power spectrum (L), a nonlinear model (NL), the standard Zeldovich approximation (Z), and two truncated linear power spectra (Ltrunc) and their associated Zeldovich approximations (Ztrunc). *Right panel:* the IGM model (2.1).

length was smaller at earlier times, which reduces the damping scale at a given redshift [31]. We can see in the right panel in Fig. 1 the strong falloff at high- k beyond the Jeans wave number $k_J \sim 20h/\text{Mpc}$. However, this is a relatively small scale effect and it does not impact the linear and weakly nonlinear growths of the IGM power spectrum.

We assume that the Lyman- α flux-decrement power spectrum $P_{\delta_F}(\mathbf{k}, z)$ can be written in terms of the IGM density power spectrum P_{IGM} as

$$P_{\delta_F}(\mathbf{k}, z) = b_{\delta_F}^2 (1 + \beta\mu^2)^2 P_{\text{IGM}}(k) / (1 + f|k\mu|/k_{\text{NL}}) e^{-(k\mu/k_{\text{th}})^2}, \quad (2.4)$$

where $\mu = \mathbf{k} \cdot \mathbf{e}_z / k$ is the cosine of the wave number direction with respect to the line of sight, b_{δ_F} the bias, β the large-scale anisotropy parameter associated with redshift-space distortions, and k_{th} the thermal broadening cutoff wave number. The anisotropic μ -dependent terms arise from redshift-space distortions, due to the amplification or damping of fluctuations measured along the line of sight because of the radial velocity fluctuations. Indeed, the mapping from real space \mathbf{x} to redshift space \mathbf{s} writes as

$$\mathbf{s} = \mathbf{x} + \frac{v_{\parallel}}{aH} \mathbf{e}_z, \quad (2.5)$$

where v_{\parallel} is the radial peculiar velocity. Then, the velocity dispersion at a given position \mathbf{x} redistributes the matter at \mathbf{x} over a nonzero width along the radial redshift-space coordinate s_{\parallel} . This leads to a smoothing of real-space density fluctuations and a damping of the redshift-space power spectrum at high k . The factor $e^{-(k\mu/k_{\text{th}})^2}$ describes the smoothing by the thermal velocity dispersion, which we take to be Gaussian with the comoving wave number cutoff

$$k_{\text{th}} = \frac{aH}{b_{\text{th}}}, \quad b_{\text{th}} = \sqrt{\frac{k_{\text{B}}T}{2m_p}}, \quad (2.6)$$

where b_{th} is the thermal velocity dispersion [33]. The factor $1/(1 + f|k\mu|/k_{\text{NL}})$ describes the smoothing by the velocity dispersion due to the virialization of collapsed structures. On nonlinear scales, beyond k_{NL} , shell crossing appears and different velocity streams coexist

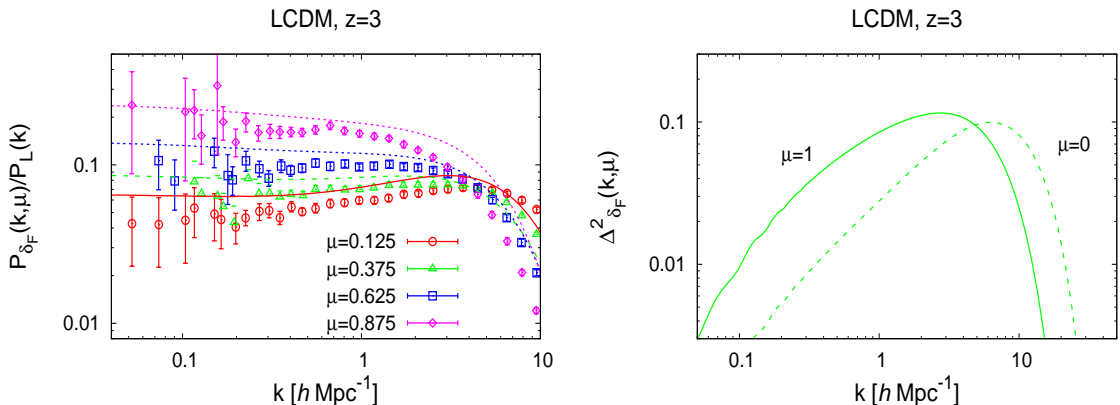


Figure 2. *Left panel:* ratio $P_{\delta_F}(k, \mu)/P_L(k)$ for $\mu = 0.125, 0.375, 0.625$ and 0.875 , from bottom to top. The symbols are the results of numerical simulations [23]. *Right panel:* logarithmic power spectrum $\Delta^2_{\delta_F}$ along the line of sight and perpendicular to the line of sight.

at the same physical space location \mathbf{x} . This must again damp the redshift-space power spectrum. The factor f expresses that this damping appears earlier when the linear velocity perturbations are amplified with respect to the linear density field. The factor $(1 + \beta\mu^2)^2$ is the usual Kaiser effect [34], which describes that on large linear scales the single-stream velocity field amplifies the density perturbations, as matter is moving inward onto overdense regions. We simply take

$$\beta \simeq 1.3 f, \quad \text{with} \quad f = \frac{d \ln D_+}{d \ln a}. \quad (2.7)$$

In principles, the factor β is defined as $\beta = f b_{\delta_F, \eta} / b_{\delta_F, \delta}$, where we distinguish the biases with respect to the linear density and velocity fields, $b_{\delta_F, \delta} = \partial \delta_F / \partial \delta$ and $b_{\delta_F, \eta} = \partial \delta_F / \partial \eta$, with $\eta = -(\partial v_{\parallel} / \partial x_{\parallel}) / (aH)$ [23, 35]. However, we found that the analytical models for $b_{\delta_F, \delta}$ and $b_{\delta_F, \eta}$ [35, 36] do not fare very well. They do not improve the agreement with numerical simulations and are not very stable, in particular the large inaccuracies on $b_{\delta_F, \eta}$ can lead to artificially large or small values for β . This agrees with the results of [36], who pointed out that velocity effects and redshift-space distortions are very difficult to capture by simple analytical models. Therefore, we keep the simple expression (2.7), which appears to be more robust. This agrees with numerical simulations, which find $\beta \sim 1.3f$ at redshift $z \simeq 3$ [23]. The prefactor $b_{\delta_F}^2$ is fitted to the observations. Apart from direct hydrodynamical simulations, an alternative would be to simulate the density and velocity fields associated with the truncated Zeldovich approximation, which allows a more accurate treatment of thermal and redshift-space distortions [25]. However, as we only wish to estimate the magnitude of the impact of modified-gravity theories, for simplicity we keep the analytical model (2.4). For precise measurements, one should in any case develop dedicated hydrodynamical simulations [26, 37, 38].

We show in the left panel in Fig. 2 the ratio of the Lyman- α power spectrum to the linear matter density power spectrum, at redshift $z = 3$ as a function of the wave number k , for several values of μ . In agreement with Eq.(2.4), higher values of μ (i.e. directions increasingly parallel to the line of sight) amplify the power spectrum on large scales, because of the Kaiser effect, and damp the power on small scales because of the μ -dependent cutoffs,

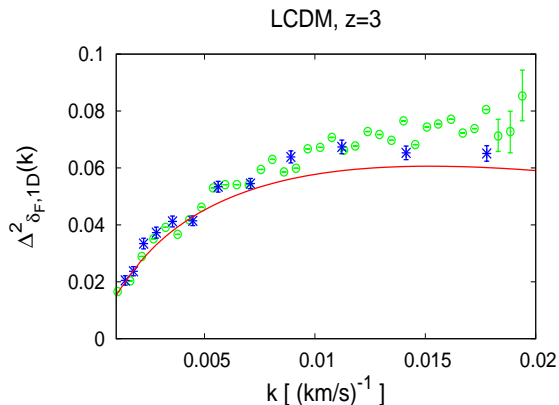


Figure 3. Logarithmic 1D power spectrum $\Delta_{\delta_F,1D}^2$. The data points are observations from [39] (circles) and [40] (stars). The solid line is our model.

due to the smoothing by the velocity dispersion that arises from the thermal distribution and the gravitational multistreaming. The agreement with the numerical simulations [23] is not perfect, as expected for such a simple model as (2.4), but we recover the main trends and the magnitude of these redshift-space distortions. This suggests that our model captures the main processes at work. We show in the right panel in Fig. 2 the logarithmic power spectrum, $\Delta_{\delta_F}^2 = 4\pi k^3 P_{\delta_F}(k, \mu)$ for $\mu = 1$ and $\mu = 0$. In agreement with the left panel, the redshift-space distortions amplify the power at low k but give rise to a steeper falloff at high k .

The expression (2.4) gives the anisotropic 3D Lyman- α power spectrum, over all directions of \mathbf{k} . The observed 1D power spectrum along the line of sight is given by the standard integral

$$P_{\delta_F,1D}(k_z) = \int_{-\infty}^{\infty} dk_x dk_y P_{\delta_F}(\mathbf{k}) = 2\pi \int_{k_z}^{\infty} dk k P_{\delta_F}(k, \mu = k_z/k). \quad (2.8)$$

This also defines the 1D logarithmic power as $\Delta_{\delta_F,1D}^2(k) = (k/\pi)P_{\delta_F,1D}(k)$, which we compare with observations [39, 40] in Fig. 3. In agreement with Fig. 2, we recover the broad shape of the observed 1D Lyman- α power spectrum. The amplitude itself is not predicted, as the bias b_{δ_F} is fitted to these observations. The lack of power at high k , $k \gtrsim 0.015$ s/km suggests some tension between the observations and the numerical simulations [23], as increasing the power at high k of the model would then worsen the agreement with the numerical simulations shown in Fig. 2. We do not tune our model to fit better the observations, to keep a reasonable agreement with both simulations and observations. This is likely to give a more robust framework. A more accurate modeling would require detailed comparisons between observations and simulations to better understand the different physical effects that enter the transformation from the linear matter density power spectrum to the Lyman- α power spectrum.

3 Modified-gravity scenarios

In this section, we use our model to estimate the sensitivity of the Lyman- α power spectrum to cosmology, more precisely to nonstandard scenarios that modify the growth of large-scale structures. We consider in turns two examples of modified-gravity models, first the $f(R)$

theories and second the K-mouflage model. We assume that the variations of the various parameters that enter Eq.(2.4) can be neglected and we evaluate the modifications to the Lyman- α power spectrum that arise from the change of the underlying matter power spectrum and the growth of structures. They enter through the nonlinear truncated Zeldovich power spectrum $P_{Z\text{trunc}}$ in Eq.(2.2), which is a function of the linear matter power spectrum and the growth rate f that sets β in Eq.(2.4).

3.1 $f(R)$ theories

We first consider the $f(R)$ -gravity theories. These models are already very strongly constrained by cosmological and astrophysical data, but they remain interesting as simple examples of modified-gravity effects on the matter distribution. Moreover, they are the only case where numerical simulations of the Lyman- α power spectrum have been performed. This allows us to check the validity of the model presented in the previous section. More specifically we concentrate on a class of $f(R)$ theories of the Hu-Sawicki [41] type, where the action is given by

$$S_{f(R)} = \frac{1}{16\pi G_N} \int d^4x \sqrt{-g} f(R) \quad (3.1)$$

with

$$f(R) = R - 2\Lambda^2 - f_{R_0} \frac{R_0^2}{R}, \quad (3.2)$$

where $\Lambda^2/8\pi G_N$ is the vacuum energy responsible for the late time acceleration of the Universe. Here R_0 is the Ricci curvature of the Universe now. We consider the case of such $f(R)$ theories with $f_{R_0} = -10^{-5}$. We show on the left panel in Fig. 4 the relative deviations of the linear and truncated Zeldovich power spectra from the Λ CDM prediction. The relative deviation grows at higher k for the linear deviation as the linear power spectrum does not include the nonlinear chameleon screening mechanism that should reduce the deviation on small scales. However, the deviation of the truncated Zeldovich power spectrum peaks at the nonlinear scale and decreases at higher k . This is due to the universal flat plateau already shown in Fig. 1. In practice, this also means that we do not need to include explicitly the nonlinear chameleon mechanism, as the deviation associated with nonlinear scales is already damped. As for the linear power spectrum, the relative deviation of the growth rate $f(k, z)$ grows with k , as seen in the right panel.

We show in Fig. 5 the deviation with respect to the Λ CDM prediction for the 3D and 1D Lyman- α power spectra. We can see in the left panel that on large linear and weakly nonlinear scales the relative deviation of the Lyman- α power spectrum grows with k , following the rise of the modification to the matter power spectrum itself. The relative deviation is greater along the radial direction, which is also sensitive to the modification of the redshift-space factor f . The relative deviation of the transverse power spectrum decreases at higher k , following the behavior of the truncated Zeldovich power spectrum. Along the radial direction, the relative deviation does not decrease at high k and goes to a finite value. This is because it remains set by the change of the overall prefactor $(1 + \beta\mu^2)^2$ in Eq.(2.4), through the modification of the growth rate f . However, this result should not be trusted at nonlinear scales, $k \gtrsim 1h/\text{Mpc}$, because this simple form of the Kaiser amplification factor only holds on linear scales. However, this range does not dominate the integral (2.8) that gives the 1D Lyman- α power spectrum.

As seen in the right panel in Fig. 5, the integration involved in the 1D Lyman- α power spectrum smoothes the relative deviation from the Λ CDM prediction. Thus, we obtain a de-

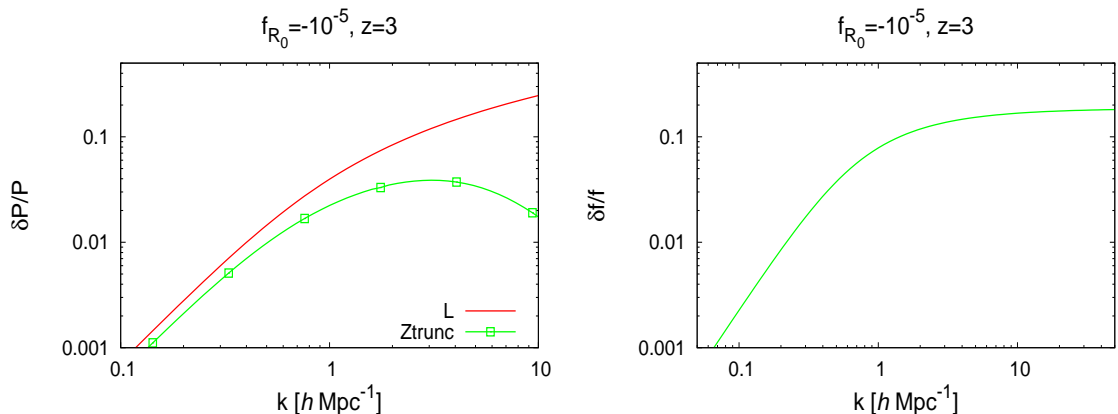


Figure 4. *Left panel:* relative deviation from the LCDM prediction of the matter power spectrum given by an $f(R)$ theory with $f_{R_0} = -10^{-5}$, at redshift $z = 3$. We show the linear power spectrum (L) and the truncated Zeldovich power spectrum (Ztrunc). *Right panel:* relative deviation of the growth rate f .

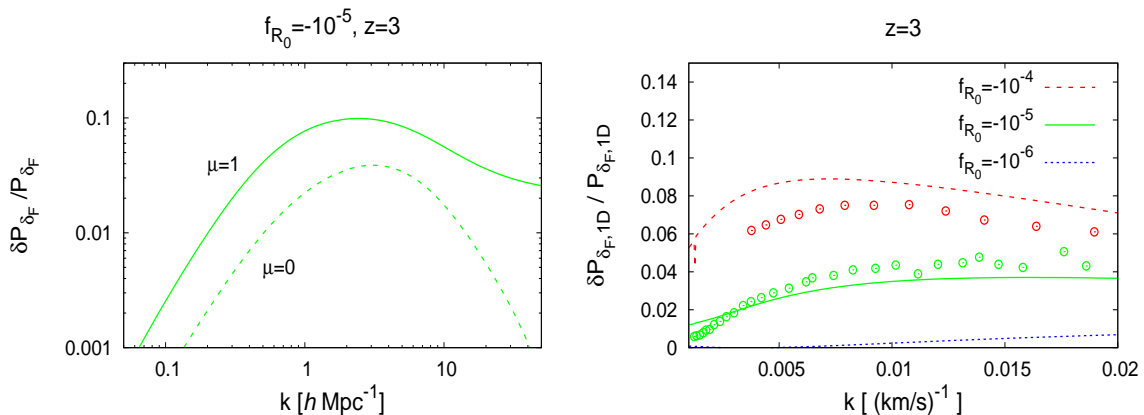


Figure 5. Relative deviation from the LCDM prediction of the Lyman- α power spectrum given by an $f(R)$ theory with $f_{R_0} = -10^{-5}$, at redshift $z = 3$. *Left panel:* 3D power spectra along directions parallel and orthogonal to the line of sight. *Right panel:* 1D power spectrum.

viation of order 4% for $f_{R_0} = -10^{-5}$, which does not vary much over $0.005 < k < 0.02 \text{ s/km}$, and a deviation of order 7% for $f_{R_0} = -10^{-4}$. Our results agree reasonably well with the numerical simulations from [13], which suggests that the model captures the main dependence on the cosmology. The modest value of the deviation from the LCDM cosmology and the lack of salient features suggest that the Lyman- α power spectrum is not a competitive tool to constrain these modified gravity models, which are already strongly constrained by astrophysical probes and Solar System tests of gravity that imply $|f_{R_0}| \lesssim 10^{-6}$. Thus, it appears that to obtain useful constraints on these scenarios one needs to reconstruct the 3D power spectrum, shown in the left panel, which shows a stronger scale dependence and a higher magnitude for the peak of the deviation from the LCDM power spectrum.

3.2 K-mouflage

We now consider the case of K-mouflage models. These are also scalar-tensor theories, but the additional scalar field is massless and has a nonstandard kinetic term. This provides another simple example of modified-gravity scenarios that includes an alternative screening mechanism. The $f(R)$ theories give rise to the chameleon screening mechanism [42, 43], where the additional scalar field obtains a higher mass in high-density environments, which decreases the range of the fifth force and screens compact objects. In contrast, the K-mouflage screening relies on a derivative screening [44–46], due to the nonlinearity of the kinetic term, so that the fifth force is damped in regions of large field gradients (or large Newtonian force), which gives rise to a K-mouflage radius around compact objects within which one recovers General Relativity. On large linear scales, from the point of view of the matter distribution, the main difference from the $f(R)$ theories is that the scalar field being massless there is no scale dependence for the linear growing mode, as in the standard LCDM cosmology, but only a time-dependent amplification.

In contrast with the $f(R)$ models, we cannot compare our results to numerical simulations, which remain to be developed. However, on linear scales the K-mouflage scenarios mostly differ from the LCDM cosmology by a time-dependent effective Newton constant, without introducing new scales. Therefore, at a qualitative level, we can expect their large-scale physics to remain even closer to the LCDM cosmology than for the $f(R)$ theories, and the model developed in section 2 should fare as well as for the $f(R)$ theories.

The K-mouflage theories are characterised by the coupling of the scalar field to matter β_K and a Lagrangian kinetic function $K(\chi)$ that is nonlinear. This function must behave like -1 when the kinetic energy of the scalar field is small in the late-time Universe, to play the role of the cosmological constant. Moreover, it must also satisfy the stringent tests of gravity in the Solar System, like the perihelion advance of the moon [47]. In this paper we take

$$K(0) = -1 \quad \text{and} \quad K'(\chi) = 1 + \frac{K_* \chi^2}{\chi^2 + \chi_*^2}, \quad (3.3)$$

where $\chi = -(\partial\phi)^2/2\mathcal{M}^4$, and \mathcal{M}^4 is the dark energy scale. The first derivative $K'(\chi)$ goes from 1 at low χ , as for the standard kinetic term, to the large value K_* at high χ , which gives rise to the screening mechanism that damps the scalar field gradients and the fifth force in high-density environments. We choose to illustrate our results with $\chi_* = 100$ and $K_* = 1000$. We consider the case of a coupling constant $\beta_K = 0.1$ (the $f(R)$ theories correspond to $\beta_f = 1/\sqrt{6}$), to remain consistent with constraints from Big Bang Nucleosynthesis and the Solar System. In practice, this gives $\bar{K}' \simeq 1$ for the background for $z \lesssim 6$, so that the precise form of $K(\chi)$ does not play any role and our results are set by the value of the coupling β_K . Indeed, in this model clusters of galaxies are still in the unscreened linear regime of the scalar field [12] and this is even more so for the Lyman- α forest clouds.

In agreement with the lack of scale dependence due to the vanishing scalar-field mass, we can see in the left panel in Fig. 6 that the relative deviation of the linear matter power spectrum is independent of wave number. The amplification of the growth of structure is due to the fifth force mediated by the scalar field and to the running of Newton’s constant with redshift, which now depends on the background value of the scalar field. As for the $f(R)$ theories shown in Fig. 4, the relative deviation of the truncated Zeldovich power spectrum decreases at high k because of its universal plateau. The relative deviation of the linear growth rate f is also scale independent. The magnitude of $\delta P/P$ and $\delta f/f$ are directly set by the coupling constant β_K .

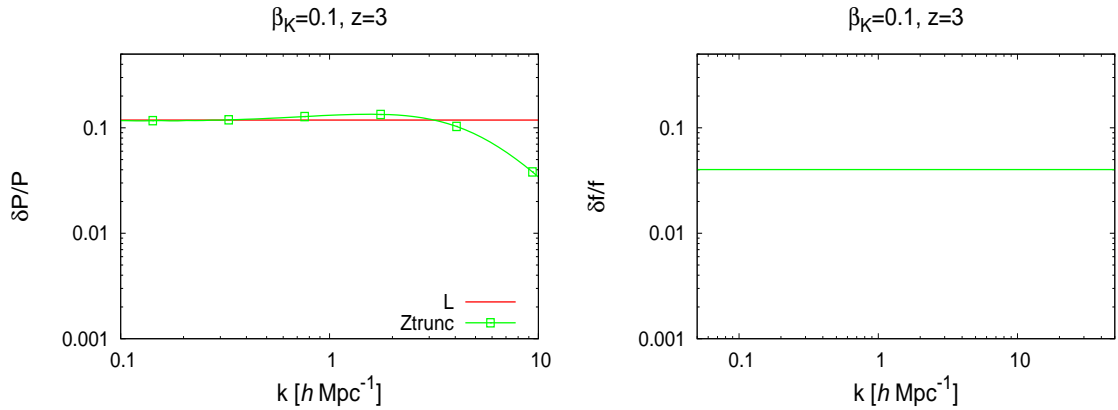


Figure 6. *Left panel:* relative deviation from the LCDM prediction of the matter power spectrum given by an $f(R)$ theory with $f_{R_0} = -10^{-5}$, at redshift $z = 3$. We show the linear power spectrum (L) and the truncated Zeldovich power spectrum (Ztrunc). *Right panel:* relative deviation of the growth rate f .

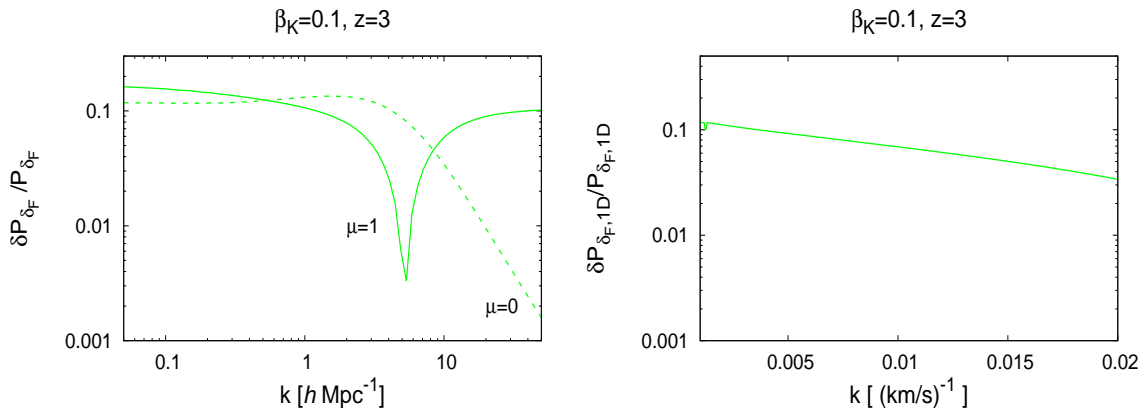


Figure 7. Relative deviation from the LCDM prediction of the Lyman- α power spectrum given by an $f(R)$ theory with $f_{R_0} = -10^{-5}$, at redshift $z = 3$. *Left panel:* 3D power spectra along directions parallel and orthogonal to the line of sight. *Right panel:* 1D power spectrum.

We present in Fig. 7 the deviation with respect to the LCDM prediction for the 3D and 1D Lyman- α power spectra. The left panel shows that on large linear and weakly nonlinear scales the relative deviation of the Lyman- α power spectrum is scale independent and it is set by the relative deviation of the linear matter power spectrum. As for the $f(R)$ scenarios, the relative deviation of the transverse power spectrum decreases at high k , following the behavior of the truncated Zeldovich power spectrum. Along the radial direction, the relative deviation shows a faster decrease and even becomes negative at high k because of the numerator in Eq.(2.4), associated with the greater velocity dispersion. Again, this behavior should not be trusted as these scales are already in the highly nonlinear regime, which is not expected to be well described by our simple modeling.

For the 1D Lyman- α flux power spectrum this gives a smooth relative deviation that slowly decrease with k . This is because of the scale independence for the relative deviation of the linear matter power spectrum, due to the zero mass of the scalar field, while at high k non-linear effects come into play that somewhat damp the dependence of the flux power spectrum on the underlying linear power spectrum. Comparing with the scatter of the observations in Fig. 3, which is of order 10%, we can estimate that a precise analysis could constrain K-mouflage models at the level of $\beta_K \lesssim 0.1$. This can be compared for instance with CMB and background constraints, which give $\beta_K \lesssim 0.2$ [48]. Therefore, in contrast with the case of the $f(R)$ theories, the Lyman- α power spectrum could provide competitive constraints for these models. This is partly due to their different screening mechanisms. In the case of K-mouflage models, the nonlinear screening that ensures convergence to General Relativity in the Solar System has not impact on weakly nonlinear cosmological scales (because this corresponds to different regimes of the kinetic function $K(\chi)$ that are not necessarily related), and the tests of gravity in the Solar System or astrophysical environments only imply $\beta_K \lesssim 0.1$ (provided $K'(\chi)$ is sufficiently large in the small-scale quasistatic regime). However, obtaining competitive constraints would require a more accurate modeling, or at least a comparison with a set of K-mouflage numerical simulations to check the accuracy of our modeling, which we leave to future work. In addition, the comparison with the case of the $f(R)$ theories shows that the shape of the relative deviation of the Lyman- α flux power spectrum can provide useful constraints on the mass of the scalar field, or more generally on whether new length scales are introduced by a possible nonstandard cosmological scenario.

4 Conclusion

In this paper, we have presented a simple modeling of the power spectrum of the Lyman- α flux decrement, which we have used to estimate the impact of two modified-gravity scenarios. We have pointed out that a Zeldovich truncated approximation provides a good starting point to describe the Lyman- α power spectrum at $z \sim 3$, as it captures weakly nonlinear structures while removing the contributions of highly nonlinear objects that do not correspond to Lyman- α forest clouds. Taking into account thermal and redshift-space effects, through bias and cutoff factors, we obtain a reasonably good agreement with numerical simulations of the concordance LCDM model and with observations.

We have then implemented this modeling for two classes of modified-gravity theories, the $f(R)$ and K-mouflage scenarios. For the $f(R)$ models, where numerical simulations are available, we obtain a reasonable agreement with the numerical results. We find that because of the line of sight integration, the deviations from the LCDM prediction for the 1D Lyman- α power spectrum are modest and flat over the observed range of wave numbers. This will make it difficult to derive competitive constraints for these models, which are already very strongly constrained by astrophysical probes. In contrast, because of their different screening mechanism, the K-mouflage models are less strongly constrained by astrophysical probes, which only constrain the negative- χ range of $K(\chi)$ with the bound $\beta_K \lesssim 0.1$. There, we find that the Lyman- α power spectrum could provide competitive constraints as compared with CMB and background measurements. However, this would require numerical simulations to check the accuracy of the analytical modeling.

In addition, the 3D Lyman- α power spectrum shows a stronger scale dependence, which is sensitive to the details of the modified-gravity theory, in particular to its scale dependence (which typically arises from the scale associated with the mass of the new scalar field). There-

fore, reconstructing the 3D power spectrum by correlating neighboring lines of sight [49–53] could provide a useful probe of alternative cosmologies.

Acknowledgments

This work is supported in part by the EU Horizon 2020 research and innovation programme under the Marie-Sklodowska grant No. 690575. This article is based upon work related to the COST Action CA15117 (CANTATA) supported by COST (European Cooperation in Science and Technology).

A The Zeldovich approximation

In the Zeldovich approximation [27], particles initially at a position \mathbf{q} evolve along a trajectory $\mathbf{x}(t, \mathbf{q})$. The variances of the relative displacement between two initial points separated by $\Delta\mathbf{q}$ are given by

$$\sigma_{\parallel}^2(\Delta q) = 2 \int d\mathbf{k} [1 - \cos(k_{\parallel} \Delta q)] \frac{k_{\parallel}^2}{\mathbf{k}^4} P_L(k) \quad (\text{A.1})$$

along the initial separation, and

$$\sigma_{\perp}^2(\Delta q) = 2 \int d\mathbf{k} [1 - \cos(k_{\perp} \Delta q)] \frac{k_{\perp}^2}{\mathbf{k}^4} P_L(k) \quad (\text{A.2})$$

in the orthogonal direction. The linear power spectrum is given by $P_L(k)$. In the Zeldovich approximation, and for Gaussian initial conditions, this leads to the Zeldovich power spectrum [28, 29]

$$P_Z(k) = \int \frac{d\Delta\mathbf{q}}{(2\pi)^3} e^{ik\mu\Delta q - \frac{1}{2}k^2\mu^2\sigma_{\parallel}^2 - \frac{1}{2}k^2(1-\mu^2)\sigma_{\perp}^2}, \quad (\text{A.3})$$

where the directing cosine is defined as $\mu = (\mathbf{k} \cdot \Delta\mathbf{q})/(k\Delta q)$. In the main text we use a truncated Zeldovich power spectrum (2.2).

References

- [1] T. Clifton, P. G. Ferreira, A. Padilla and C. Skordis, *Modified Gravity and Cosmology*, *Phys. Rep.* **513** (2012) 1 [1106.2476].
- [2] S. F. Hassan and R. A. Rosen, *Bimetric Gravity from Ghost-free Massive Gravity*, *JHEP* **02** (2012) 126 [1109.3515].
- [3] C. de Rham, G. Gabadadze and A. J. Tolley, *Resummation of Massive Gravity*, *Phys. Rev. Lett.* **106** (2011) 231101 [1011.1232].
- [4] E. Babichev, C. Charmousis, G. Esposito-Farèse and A. Lehébel, *Stability of black holes and the speed of gravitational waves within self-tuning cosmological models*, *Phys. Rev. Lett.* **120** (2018) .
- [5] G. W. Horndeski, *Second-order scalar-tensor field equations in a four-dimensional space*, *Int.J.Theor.Phys.* **10** (1974) 363.
- [6] C. Deffayet, X. Gao, D. Steer and G. Zahariade, *From k-essence to generalised Galileons*, *Phys. Rev. D* **D84** (2011) 064039 [1103.3260].
- [7] J. Gleyzes, D. Langlois, F. Piazza and F. Vernizzi, *Healthy theories beyond Horndeski*, *Phys. Rev. Lett.* **114** (2015) 211101 [1404.6495].

- [8] P. Creminelli and F. Vernizzi, *Dark Energy after GW170817 and GRB170817A*, *Phys. Rev. Lett.* **119** (2017) 251302 [[1710.05877](#)].
- [9] Y. Akrami, P. Brax, A.-C. Davis and V. Vardanyan, *Neutron star merger gw170817 strongly constrains doubly coupled bigravity*, *Phys. Rev. D* **97** (2018) .
- [10] L. Lombriser, *Constraining chameleon models with cosmology*, *Annalen der Physik* **526** (2014) 259.
- [11] P. Brax and P. Valageas, *K-mouflage Cosmology: the Background Evolution*, *Phys. Rev. D* **90** (2014) 023507 [[1403.5420](#)].
- [12] P. Brax, L. A. Rizzo and P. Valageas, *K-mouflage effects on clusters of galaxies*, *Phys. Rev. D* **92** (2015) 043519 [[1505.05671](#)].
- [13] C. Arnold, E. Puchwein and V. Springel, *The Lyman α forest in $f(R)$ modified gravity*, *Month. Not. Roy. Astron. Soc.* **448** (2015) 2275 [[1411.2600](#)].
- [14] V. K. Narayanan, D. N. Spergel, R. Davé and C.-P. Ma, *Constraints on the mass of warm dark matter particles and the shape of the linear power spectrum from the lyman α forest*, *Astroph. J.* **543** (2000) L103.
- [15] M. Viel, G. D. Becker, J. S. Bolton and M. G. Haehnelt, *Warm dark matter as a solution to the small scale crisis: New constraints from high redshift lyman- α forest data*, *Phys. Rev. D* **88** (2013) .
- [16] J. Baur, N. Palanque-Delabrouille, C. Yèche, C. Magneville and M. Viel, *Lyman-alpha forests cool warm dark matter*, *JCAP* **2016** (2016) 012.
- [17] V. Iršič, M. Viel, M. G. Haehnelt, J. S. Bolton and G. D. Becker, *First constraints on fuzzy dark matter from lyman- α forest data and hydrodynamical simulations*, *Phys. Rev. Lett.* **119** (2017) .
- [18] M. Garny, T. Konstandin, L. Sagunski and S. Tulin, *Lyman- α forest constraints on interacting dark sectors*, *JCAP* **2018** (2018) 011.
- [19] R. A. C. Croft, D. H. Weinberg, N. Katz and L. Hernquist, *Recovery of the power spectrum of mass fluctuations from observations of the lyman α forest*, *Astroph. J.* **495** (1998) 44.
- [20] R. A. C. Croft, D. H. Weinberg, M. Bolte, S. Burles, L. Hernquist, N. Katz et al., *Toward a precise measurement of matter clustering: Lyman α forest data at redshifts 2-4*, *Astroph. J.* **581** (2002) 20.
- [21] P. McDonald, *Toward a measurement of the cosmological geometry at $z \sim 2$: Predicting lyman α forest correlation in three dimensions and the potential of future data sets*, *Astroph. J.* **585** (2003) 34.
- [22] P. McDonald, U. Seljak, R. Cen, D. Shih, D. H. Weinberg, S. Burles et al., *The linear theory power spectrum from the lyman α forest in the sloan digital sky survey*, *Astroph. J.* **635** (2005) 761.
- [23] A. Arinyo-i Prats, J. Miralda-Escudé, M. Viel and R. Cen, *The non-linear power spectrum of the lyman alpha forest*, *JCAP* **2015** (2015) 017.
- [24] H. Bi and A. F. Davidsen, *Evolution of structure in the intergalactic medium and the nature of the lyman α forest*, *Astroph. J.* **479** (1997) 523.
- [25] L. Hui, N. Y. Gnedin and Y. Zhang, *The statistics of density peaks and the column density distribution of the lyman α forest*, *Astroph. J.* **486** (1997) 599.
- [26] S. Peirani, D. H. Weinberg, S. Colombi, J. Blaizot, Y. Dubois and C. Pichon, *Lyman- α forest: Predicting large-scale lyman α forest statistics from the dark matter density field*, *Astroph. J.* **784** (2014) 11.
- [27] Y. B. Zel'Dovich, *Gravitational instability: An approximate theory for large density perturbations.*, *Astron. and Astrophys.* **5** (1970) 84.

- [28] P. Schneider and M. Bartelmann, *The power spectrum of density fluctuations in the Zel'dovich approximation*, *Month. Not. Roy. Astron. Soc.* **273** (1995) 475.
- [29] A. N. Taylor and A. J. S. Hamilton, *Non-linear cosmological power spectra in real and redshift space*, *Month. Not. Roy. Astron. Soc.* **282** (1996) 767 [[arXiv:astro-ph/9604020](#)].
- [30] P. Coles, A. L. Melott and S. F. Shandarin, *Testing approximations for non-linear gravitational clustering*, *Month. Not. Roy. Astron. Soc.* **260** (1993) 765.
- [31] N. Y. Gnedin and L. Hui, *Probing the universe with the Lyman α forest – i. hydrodynamics of the low-density intergalactic medium*, *Month. Not. Roy. Astron. Soc.* **296** (1998) 44.
- [32] M. Zaldarriaga, R. Scoccimarro and L. Hui, *Inferring the Linear Power Spectrum from the Lyman α Forest*, *Astroph. J.* **590** (2003) 1 [[arXiv:astro-ph/0111230](#)].
- [33] A. Garzilli, T. Theuns and J. Schaye, *The broadening of Lyman- α forest absorption lines*, *Month. Not. Roy. Astron. Soc.* **450** (2015) 1465 [[1502.05715](#)].
- [34] N. Kaiser, *Clustering in real space and in redshift space*, *Month. Not. Roy. Astron. Soc.* **227** (1987) 1.
- [35] U. Seljak, *Bias, redshift space distortions and primordial nongaussianity of nonlinear transformations: application to Lyman- α forest*, *JCAP* **2012** (2012) 004.
- [36] A. M. Cieplak and A. Slosar, *Towards physics responsible for large-scale Lyman- α forest bias parameters*, *JCAP* **2016** (2016) 016.
- [37] G. Rossi, N. Palanque-Delabrouille, A. Borde, M. Viel, C. Yèche, J. S. Bolton et al., *Suite of hydrodynamical simulations for the Lyman- α forest with massive neutrinos*, *Astron. and Astrophys.* **567** (2014) A79 [[1401.6464](#)].
- [38] C. Lochhaas, D. H. Weinberg, S. Peirani, Y. Dubois, S. Colombi, J. Blaizot et al., *Modelling Lyman α forest cross-correlations with Lyman- α forest*, *Month. Not. Roy. Astron. Soc.* **461** (2016) 4353.
- [39] N. Palanque-Delabrouille, C. Yèche, A. Borde, J.-M. Le Goff, G. Rossi, M. Viel et al., *The one-dimensional Lyman α forest power spectrum from BOSS*, *Astron. and Astrophys.* **559** (2013) A85.
- [40] P. McDonald, U. Seljak, S. Burles, D. J. Schlegel, D. H. Weinberg, R. Cen et al., *The Lyman α forest power spectrum from the Sloan Digital Sky Survey*, *Astroph. J. Supplement Series* **163** (2006) 80.
- [41] W. Hu and I. Sawicki, *Models of $f(R)$ Cosmic Acceleration that Evade Solar-System Tests*, *Phys. Rev.* **D76** (2007) 064004 [[0705.1158](#)].
- [42] J. Khoury and A. Weltman, *Chameleon fields: Awaiting surprises for tests of gravity in space*, *Phys. Rev. Lett.* **93** (2004) 171104 [[astro-ph/0309300](#)].
- [43] J. Khoury and A. Weltman, *Chameleon Cosmology*, *Phys. Rev.* **D69** (2004) 044026 [[astro-ph/0309411](#)].
- [44] E. Babichev, C. Deffayet and R. Ziour, *k -Mouflage gravity*, *Int.J.Mod.Phys.* **D18** (2009) 2147 [[0905.2943](#)].
- [45] P. Brax, C. Burrage and A.-C. Davis, *Screening fifth forces in k -essence and DBI models*, *JCAP* **01** (2013) 20 [[1209.1293](#)].
- [46] P. Brax and P. Valageas, *K -mouflage cosmology: The background evolution*, *Phys. Rev. D* **90** (2014) 023507 [[1403.5420](#)].
- [47] A. Barreira, P. Brax, S. Clesse, B. Li and P. Valageas, *K -mouflage gravity models that pass solar system and cosmological constraints*, *Phys. Rev. D* **91** (2015) .

- [48] G. Benevento, M. Raveri, A. Lazanu, N. Bartolo, M. Liguori, P. Brax et al., *K-mouflage Imprints on Cosmological Observables and Data Constraints*, *ArXiv e-prints* (2018) [[1809.09958](#)].
- [49] C. Pichon, J. Vergely, E. Rollinde, S. Colombi and P. Petitjean, *Inversion of the lyman α forest: three-dimensional investigation of the intergalactic medium*, *Month. Not. Roy. Astron. Soc.* **326** (2001) 597.
- [50] A. Slosar, A. Font-Ribera, M. M. Pieri, J. Rich, J.-M. L. Goff, É. Aubourg et al., *The lyman- α forest in three dimensions: measurements of large scale flux correlations from boss 1st-year data*, *JCAP* **2011** (2011) 001.
- [51] J. Cisewski, R. A. C. Croft, P. E. Freeman, C. R. Genovese, N. Khandai, M. Ozbek et al., *Non-parametric 3d map of the intergalactic medium using the lyman-alpha forest*, *Month. Not. Roy. Astron. Soc.* **440** (2014) 2599.
- [52] M. Ozbek, R. A. C. Croft and N. Khandai, *Large-scale 3d mapping of the intergalactic medium using the lyman α forest*, *Month. Not. Roy. Astron. Soc.* **456** (2016) 3610.
- [53] A. Font-Ribera, P. McDonald and A. Slosar, *How to estimate the 3d power spectrum of the lyman- α forest*, *JCAP* **2018** (2018) 003.